Hindawi
Geofluids
Volume 2018, Article ID 3015038, 12 pages
https://doi.org/10.1155/2018/3015038

Research Article

Microscale Research on Effective Geosequestration of CO_2 in Coal Reservoir: A Natural Analogue Study in Haishiwan Coalfield, China

Kaizhong Zhang,[1,2,3] Wei Li ,[1,2,3] Yuanping Cheng ,[1,2,3] Jun Dong,[1,2,3] Qingyi Tu,[1,2,3] and Rong Zhang[1,2,3]

[1]*Key Laboratory of Coal Methane and Fire Control, Ministry of Education, China University of Mining and Technology, Xuzhou, Jiangsu 221116, China*
[2]*National Engineering Research Center of Coal Gas Control, China University of Mining & Technology, Xuzhou, Jiangsu 221116, China*
[3]*School of Safety Engineering, China University of Mining and Technology, Xuzhou 221116, China*

Correspondence should be addressed to Wei Li; weilcumt@hotmail.com and Yuanping Cheng; cyp620924@outlook.com

Received 1 October 2017; Revised 29 January 2018; Accepted 4 February 2018; Published 28 February 2018

Academic Editor: Marco Petitta

A natural analogue study in CO_2-rich coalfield (Haishiwan, China) provides a strong support for safe, reliable, and long-term storage by analyzing the mechanism of CO_2 migration, entrapment, and storage in coal reservoir. Thus, effects of geological tectonism on reservoir properties were investigated. Simultaneously, coal and oil shale samples before and after supercritical CO_2 ($SCCO_2$) treatment via geochemical reactor were collected to analyze changes in pore structure, functional group distributions, and $SCCO_2$ extraction. Observations from in situ properties of coal seam indicate that there is a positive relationship with CH_4 contents and F19 fault whereas CO_2 and carbonate contents decrease as the distance from F19 increases. Analysis of pore properties reveals that $SCCO_2$ enlarges the development of coal pore and facilitates the diffusion and seepage channel of coal reservoir, while no changes in larger pores are found in oil shale, which may restrain fluids from passing through. Then, oxygen-containing functional groups are mobilized by $SCCO_2$ from oil shale, associated with a decrease in sorption sites. The sealing capacity of cap rock (oil shale) and geological tectonism (F19 fault), as the major contributors to CO_2 enrichment and accumulation, provides insights into the suitable selection of CCGS site for long geological time.

1. Introduction

Atmospheric CO_2 originates mainly from fossil fuel combustion, which is responsible for about 70% of the greenhouse effect [1, 2]. China's CO_2 emissions in 2016 continue to be number one in the world with 27.3% of total [3]. To reduce anthropogenic CO_2 emissions, CCGS is put forward as a promising approach by CO_2 capture, transport, and injection into a storage site, such as depleted oil and gas reservoirs, saline aquifers, and unmineable coal seams [4–6]. As one of the most common potential disposal sites, CO_2 geological storage in coal mines has a significant meaning related to CO_2-enhanced coalbed methane (ECBM) recovery [7]. However, storage in coal seam faces tremendous challenges: (1) the potential geological risks related to seismicity and ground movement in unstable coal reservoirs; (2) the health, safety, and environmental risks causing CO_2 leakage to cap rock, tectonic zone, and fractures [8, 9]. Therefore, special attention should be given on the effective and safe storage of CO_2 in suitable sites, with the purpose of CO_2 leakage control, which serves as a primary risk factor.

In fact, only several pilot CCGS projects have been conducted and it is apparent that CO_2 storage in coal is not widely accepted in China [10]. A knowledge on CO_2 behavior of long-term storage is limited for the field experiments in coalfields [11]. Previous studies have been demonstrated that CO_2 in Yaojie coalfield can be naturally stored over long geological period under suitable conditions [12]. To some extent, the presence of CO_2 in Yaojie coalfield can be analogous to long-term storage of CO_2, which may yield insights

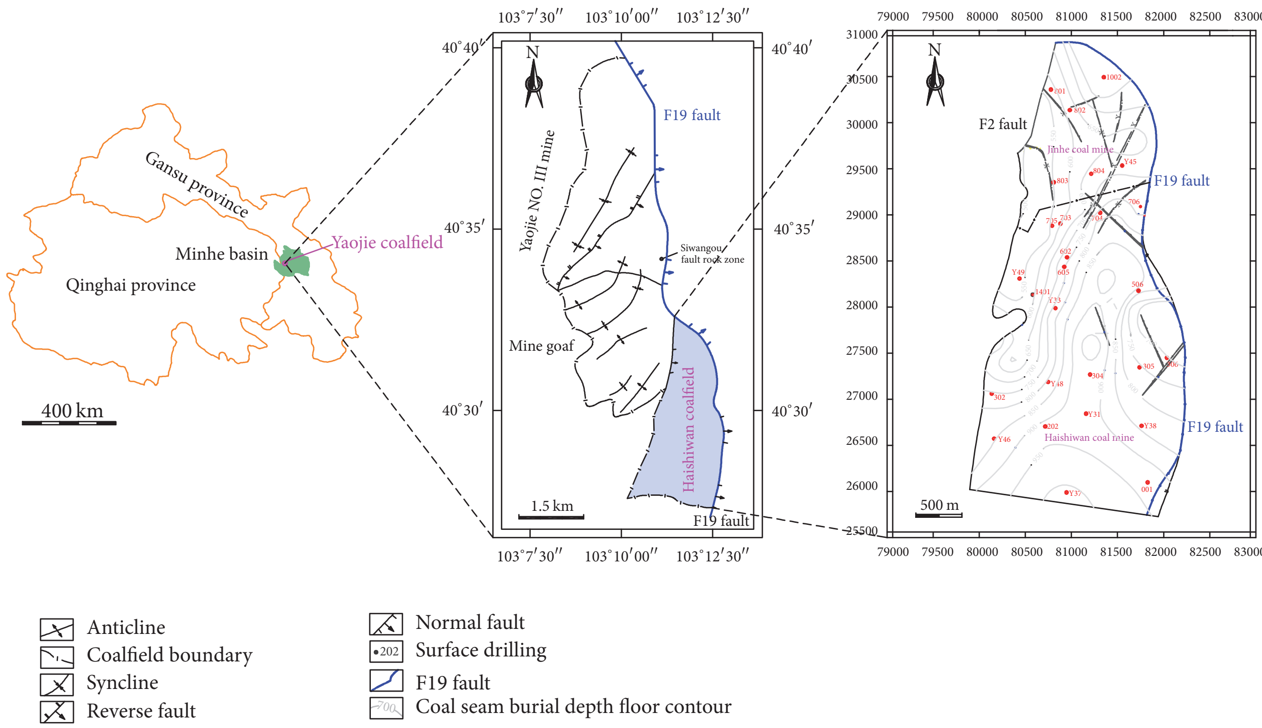

Figure 1: Geographical location of Yaojie coalfield and exploration of surface borehole in Haishiwan coalfield.

into the mechanisms of CO_2 migration, entrapment, and storage in coal reservoirs. Therefore, the suitability of CO_2 injection sites and other activities in this area need to be fully considered from the macroscopic and microscopic views.

From the macroscopic view, a group of geological factors including occurrence of coal seam, subsurface condition, cap rock types, and regional tectonic condition should be analyzed and evaluated [13–15]. The microscopic view refers to the interactions between CO_2 and rocks (coal or cap rock) and the effects of CO_2 on the physical (structure of pore or fracture) and chemical (molecules) properties [16]. For coal, the interactions with CO_2 are generally divided into three categories: (1) swelling effect, caused by CO_2 absorbing into coal matrix, leading to a decrease in the fracture aperture and permeability of coal reservoir [17, 18]; (2) the transformation and rearrangement of coal structure after $SCCO_2$ treatment [19, 20]; (3) $SCCO_2$ extraction of organic matter and inorganic material in coal, accompanied by the existence of water [21]. Although the above findings have been published in the literature over the past decade in the area of CCGS, a knowledge gap exists on the effects of $SCCO_2$ on cap rocks, that is, oil shale in this study. In Haishiwan coalfield, the roof of coal seam is enclosed by a mass of oil shale, which serves as a better sealant for $SCCO_2$ pressure [12]. Actually, cap rock, one of the most important factors, dominates the sealing capacity of coal reservoirs [22]. Hence, an effort should be made to study the changes of oil shale structure after $SCCO_2$ treatment.

The main purpose of this study is to investigate the feasibility of effective and safe geological sequestration of CO_2 in coal seams underling cap rock (oil shale), which takes Haishiwan coal seam in China with high CO_2 content as a natural analogue. A knowledge of the mechanisms of CO_2 migration, entrapment, and storage in Haishiwan coalfield contributes to a better understanding of long-term storage of CO_2 in the field of CCGS. Therefore, the structure in this paper is as follows. Firstly, geological factors related to tectonism and its influence on in situ properties of coal seam were investigated and analyzed. Subsequently, samples of coal and oil shale were treated by $SCCO_2$ geochemical reactor to perform comparative tests, including pore properties, functional group distributions, and Gas Chromatography-Mass Spectrum (GC-MS) analysis. Then, the mechanisms of CO_2 migration, entrapment, and storage were discussed to demonstrate how to effectively and safely store CO_2 in coalfield.

2. Regional Geology

2.1. Geological Setting of Yaojie Coalfield. As shown in Figure 1, Yaojie coalfield, as a secondary tectonic unit in Minhe basin, is located in the west margin of Gansu and Qinghai provinces. There are many well-developed faults and constructions in Minhe, which is a Mesozoic–Cenozoic mountain depression basin expanded by the Qilian orogenic belt. The tectonic evolution of Minhe basin is composed of Indosinian movement, Yanshan movement, and Himalayan movement, resulting in the basin formation and transformation. Yaojie coalfield belongs to middle Jurassic coal-bearing series in Mesozoic. The strike, dip, and area are 2.6 km, 11 km, and 28.6 km^2, respectively. The coal bearing basin extended in a NNW direction with the F19 fault zone located to the east of it. Yaojie coalfield, belonging to the Yaojie Coal-Electricity Corporation, consists of Zhangergou coal mine, Yaojie NO. III coal mine, Jinhe coal mine, and Haishiwan coal

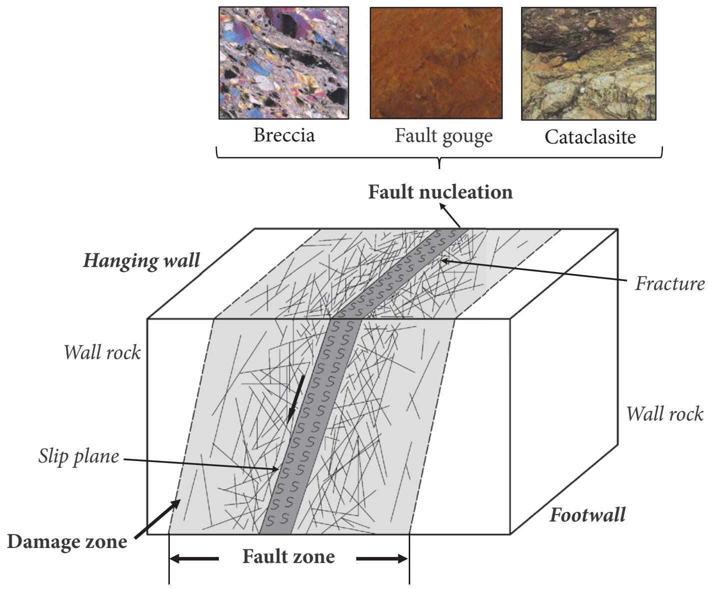

Figure 2: Structure diagram of ductile shear fault.

mine. Haishiwan coalfield, as a concealed coalfield, is located in the south of Yaojie coal fields in Minhe basin. The main coal seam containing CO_2 is No. 2 coal seam; the average thickness of which is 20 m with thicker in the west and thin in the east. The roof of No. 2 coal seam is carbon mudstone, siltstone, and oil shale. The floor of No. 2 coal seam is carbon mudstone.

2.2. F19 Faults. There is no direct evidence exactly to show the formation time of CO_2 fluids were affected by F19 faults, but the isotopic age chlorite thermal alteration and the fission track age of the calcite veins of ultrabasic have proved that CO_2 hydrothermal activity was concentrated in this period [12]. In Neogene period with Himalayan movement, F19 fault was a tensional activity period, the permeability and fluid potential of which increased with the possibility of the upward migration of CO_2 fluids [23]. Therefore, CO_2 fluids were mainly formed in Neogene period. Whereafter, fault tensional activity quitted or transformed into pressure shear state, making the vertical migration of CO_2 fluids slow down to stagnation. Up to the present, the vertical closure and principal compressive stress of NE direction suggest F19 fault has been still in a closed state. For this area, ductile shear fault is classified as damage zone and fault nucleation zone, which is presented in Figure 2. The fault nucleation was filled with breccia, fault gouge, and cataclasite, and the old faults have been blocked by quartz, calcite, and zeolite, which could result in a poor permeability in F19 fault. However, there are amount of minor faults and fractures in damage zone, indicating that good permeability in this area may be the main lateral migration channel of CO_2 fluids.

2.3. Sources of CO_2. It has been proven that CO_2 of Earth's crust derived from stratal carbonate pyrolysis generating inorganic CO_2, which are influenced by contact metamorphism of carbonates and dynamic metamorphism of fault activities [24]. According to geological survey in Geological Institute (Gansu, China), magmatic intrusion has never happened in the region since the Paleozoic [25]. Therefore, the possibility of contact metamorphism can be excluded during inorganic CO_2 generating process. However, due to the existence of F19 fault, the fault zone tends to suffer intense extrusion and shear, leading to the hydrothermal activities with structural and tectonic characteristics [26]. Given that carbonate rocks in active fault zone may result in dynamometamorphism under the effect of ductile-brittle shearing action, element differentiation may occur and CO_2 will be generated after migration [27]. This is the main formation mechanism of inorganic CO_2 in this region.

3. Experimental Section

3.1. Sample Preparation. Coal samples were sampled from the air-return way of coalface in Haishiwan coal mine, while oil shale samples were derived from the roof of No. 2 coal seam. The samples were immediately sealed and sent to the laboratory as soon as possible to prevent oxidation. Subsequently, the samples were crushed and screened to the appropriate quantity and sizes for each test. Before tests, samples were dried at 80°C for 48 h using turbo molecular pump vacuum.

Following China National Standard GB/T 212-2008, proximate analyses of moisture, ash, and volatile matter were performed using a 5E-MAG6600 proximate analyzer (Changsha Kaiyuan Instruments, China). The mean maximum reflectance of vitrinite ($R_{o,max}$, %) was determined using a Zeiss microscope-photometer (German) following China National Standard GB/T 6948-2008. The basic properties of the coal and oil shale samples are listed in Table 1.

3.2. $SCCO_2$ High-Pressure Geochemical Reactor. To better understand the changes in physical and chemical structure, the samples (coal and oil shale) before and after $ScCO_2$ treatment were conducted by $SCCO_2$ high-pressure geochemical

Table 1: Basic properties of the coal and oil shale samples.

Sample	M_{ad} (%)	A_d (%)	V_{ad} (%)	$R_{o,max}$ (%)
Coal	1.84	5.91	28.45	0.96
Oil shale	1.31	5.51	26.38	0.62

Note. M_{ad} means the moisture content (air-dried basis), A_d means the ash content (dried basis), V_{ad} means the volatile matter content (air-dried basis), and $R_{o,max}$ means the maximum vitrinite reflectance.

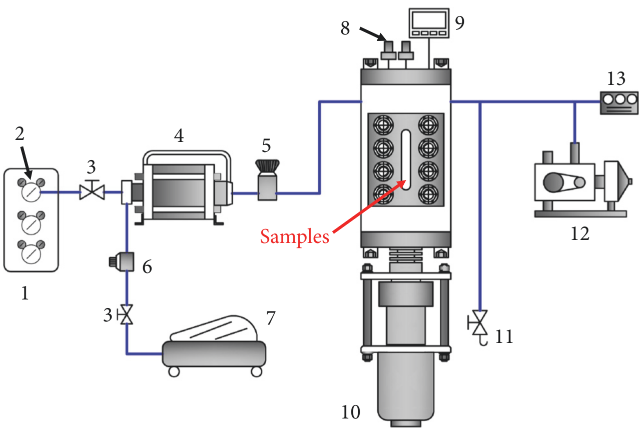

Figure 3: Schematic of $SCCO_2$ high-pressure geochemical reactor simulating CO_2 injection. (1) Gas supply; (2) reducing valve; (3) valve; (4) gas booster pump; (5) reducing valve; (6) pressure regulating valve; (7) air compressor; (8) temperature and pressure transducers; (9) temperature and pressure indicator; (10) $SCCO_2$ high-pressure geochemical reactor; (11) safety valve; (12) vacuum pump; (13) vacuum gauge.

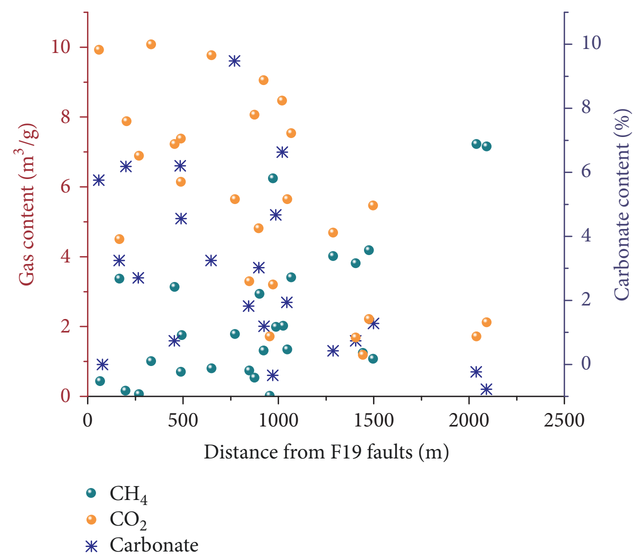

Figure 4: Changes of CO_2 and carbonate distributions as the distance from F19 increases.

reactor, which can simulate CO_2 injection in the reservoir (Figure 3). Firstly, samples were degassed in the vacuum pump system (60°C and 4 Pa for 48 h). Secondly, CO_2 was injected to pipeline while air compressor started to provide power. 10 min later, gas booster pump was opened and then high-pressure CO_2 was filled in the reactor. Eventually, the pressure and temperature of reaction were set at 10 MPa and 50°C, respectively, and the reaction time is 360 h. Actually, This condition could not lead to chemical degradation of the coal matrix [28]. To some degree, the pressure-temperature conditions in this study were used to simulate CO_2 sequestration scenarios in coal beds (1 km depth), though it could not be representative of CO_2 sequestration in deep coal beds based on field [28].

3.3. Experimental Methods. Pore structure analysis of macropore was performed using A PoreMaster 33 automated mercury intrusion porosimeter (Quantachrome Instruments, United States), which could effectively measure pore diameters of 6 to 100 μm over a pressure range from 0.14 to 215 MPa. The mesopore and micropore analysis were obtained using an AUTOSORB-1 (Quantachrome Instruments, United States). With these two methods, specific surface area (SSA), total pore volume (TPV), pore size distributions (PSDs), and porosity of micropores, mesopores, and macropores can be precisely analysed.

GC-MS analysis was conducted by a Hewlett–Packard 6890/5973 GC/MS associated with a capillary column applied with HP-5MS (cross-link 5% PH MEsiloxane, 30 m × 0.25 mm i.d., 0.25 mm film thickness), a quadrupole analyzer, and operated in electron-impact (70 eV) mode. The data can be performed automatically by Chemstation software. The compounds were characterized by comparing mass spectra according to NIST05 library data.

FTIR spectra of the samples were measured using a device that combined a VERTEX 80 Fourier transform infrared spectrometer with a HYPERION 2000 infrared microscope (Bruker, Germany) at a resolution of 0.06 cm^{-1} and spectral region of 8000–350 cm^{-1}.

4. Results

4.1. Relationships with F19 Fault, CO_2, and Carbonate Distributions. Figure 1 exhibits the locations of 28 surface boreholes for the No. 2 coal seam during geological exploration period in Haishiwan coalfield. Gas (CO_2, CH_4) and carbonate mineral contents were obtained from surface borehole coal samples, which were shown in Figure 4.

The on-site CO_2 contents are between 0.3 m^3/g and 10 m^3/g, whereas CH_4 contents are between 0.03 m^3/g and 7.23 m^3/g. Then, a negative correlation was found between CO_2 contents and the distance from F19 faults, while it seems

Table 2: Pore structure analyses of the oil shale and coal sample.

Sample	Measurement of micropores with CO_2 adsorption		Measurement of mesopores with N_2 adsorption		Measurement of macropores with MIP		
	DFT-TPV (mL/g)	DFT-SSA (m^2/g)	BJH-TPV (mL/g)	BET-SSA (m^2/g)	MIP-TPV (mL/g)	MIP-SSA (m^2/g)	Porosity (%)
Oil shale	0.023	89.17	0.0018	3.43	0.0076	1.95	2.31
Coal	0.076	187.51	0.0054	6.92	0.017	2.23	5.82

Note. The sample weight is on an air-dried basis. SSA refers to specific surface area; TPV refers to total pore volume.

to be a positive correlation between CH_4 contents and F19 faults. Because CO_2 molecule has stronger capacity to diffuse and adsorb than CH_4 molecule, the highest content of CO_2 may be found near F19 faults. That is, it can be regarded as the input of CO_2. It is summarized that CH_4 in the coal seam will be recovered after CO_2 sequestration through CO_2 injection.

The distribution of carbonate mineral ranges from 0.2% to 9.7%. The data in Figure 4 suggests that carbonate contents decrease with increasing distance from F19 fault. According to the literature, carbonate, as a tracing mineral of inorganic CO_2 migration, is related to the existence of water, pH value, pressure, and former mineral [29]. The distribution of carbonate mineral indicates that under a certain condition CO_2 is likely to transform into carbonate minerals near the F19 fault zone.

4.2. Pore Characteristics. Studies on the pore structure of oil shales and coals indicate the development and connectivity of smaller pores (micropores) and larger pores (macropores) directly relate to the desorption, diffusion, and seepage, respectively [30, 31]. The International Union of Pure and Applied Chemistry (IUPAC) classified pores into micropores (<2 nm), mesopores (2–50 nm), and macropores (>50 nm), which is widely recognized by the scholars [32].

For mesopores, N_2 adsorption at 77 K can be regarded as the standard method to determine TPV and SSA using the Barrett–Joyner–Halenda (BJH) and Brunauer–Emmett–Teller (BET) models, respectively [32–34]. For micropores, CO_2 adsorption at 273 K may overcome the disadvantages that N_2 adsorption is inaccessible to ultramicropores (<0.7 nm), which can be interpreted by the density functional theory (DFT) analyses for TPV and SSA [35, 36]. In this study, physisorption method (N_2/CO_2 adsorption) can be automatically analyzed by the ASiQwin computer software from Quantachrome (United States). However, physisorption method is not suitable for larger macropores (>300 nm) analysis [37]. Thus, mercury intrusion porosimetry (MIP) is more effective for TPV and SSA of macropores through PoreMaster from Quantachrome (United States).

As shown in Table 2, in general, micropores volume and surface area of oil shale and coal samples occupy a large proportion in total pore volume. However, there is less development of macropores, mesopores, and micropores in oil shale, compared to coal sample. Especially for MIP, the porosity of coal is 5.82%, which seems to be more than twice as large as oil shale of 2.31%. It may indicate that coal has a better migration channel than oil shale, due to a more complex and developed pore structure. Also, the SSA of micropores dominate in coal, compared with oil shales, suggesting that the most fluid molecules (CH_4 or CO_2) can be inclined to adsorb and store in micropores.

Generally, the PSD of micropore and lower pore size range of mesopore can be characterized by N_2 adsorption using DFT method [38, 39]. MIP with a function of Incremental pore volume and pore diameter can reflect the PSD of larger pore size range mesopore and macropore. These methods show a good representation from micropore to macropore, which almost cover the whole range of PSDs.

Figure 5 depicts the PSDs of untreated and $SCCO_2$-treated oil shale. No obvious changes were observed in the PSD of MIP, especially in the PSD of macropores. This indicates that $SCCO_2$ has little influence on the larger pores (mesopore and macropore) of oil shale. The inset in Figure 5 highlights that smaller pores (micropore and mesopore) decrease obviously after $SCCO_2$ treatment, suggesting that $SCCO_2$ may alter the inherent structure of oil shale by reducing the TPV [40]. The decrease in micropores and mesopores may be attributed to the adsorption-induced deformation in pores after $SCCO_2$ treatment [41]. Figure 6 shows the PSDs of coal before and after $SCCO_2$ treatment. Unlike the PSD of oil shale, the PSDs of coal in Figure 6 exhibit a bipolar distribution, which contains more micropores and macropores, and mesopores are not developed in coal. This may indicate that coal has a strong ability for gas desorption, diffusion, and seepage, compared with oil shale. Furthermore, the PSD of MIP after $SCCO_2$ treatment shows more macropores and mesopores than untreated coal sample, except for the pore diameter range around 100 nm. For DFT method, two well-defined peaks and some of disorderly peaks are found in micropores and mesopores, suggesting the well-developed micropores in coal structure and better adsorbed ability. With $SCCO_2$ treatment, micropores and mesopores show an increase in the PSDs of DFT method. Eventually, $SCCO_2$ promotes the development of micropores, mesopores, and macropores in coal, which may facilitate the movement of fluids from the coal matrix via desorption and diffusion and transport in the fracture via seepage.

The cumulative pore volume curves of the untreated and $SCCO_2$-treated oil shale analyzed by MIP are displayed in Figure 7. In general, the concave shape is shown in the ejection curves, which may result from a mass of open pores and semiclosed pores. This may contribute to the connectivity

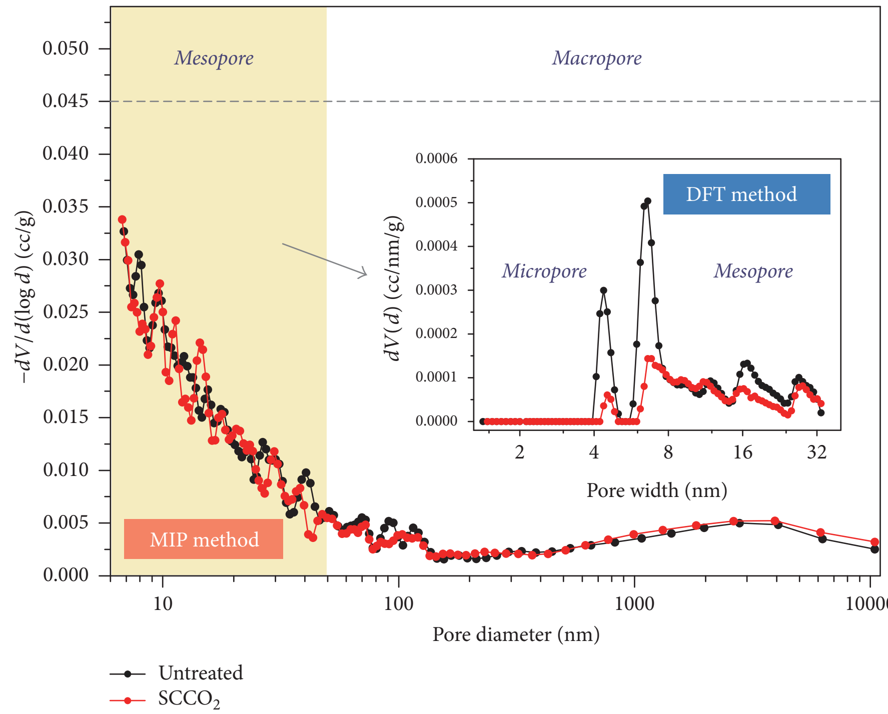

Figure 5: Pore size distribution of untreated and $SCCO_2$-treated oil shale from the MIP and DFT method.

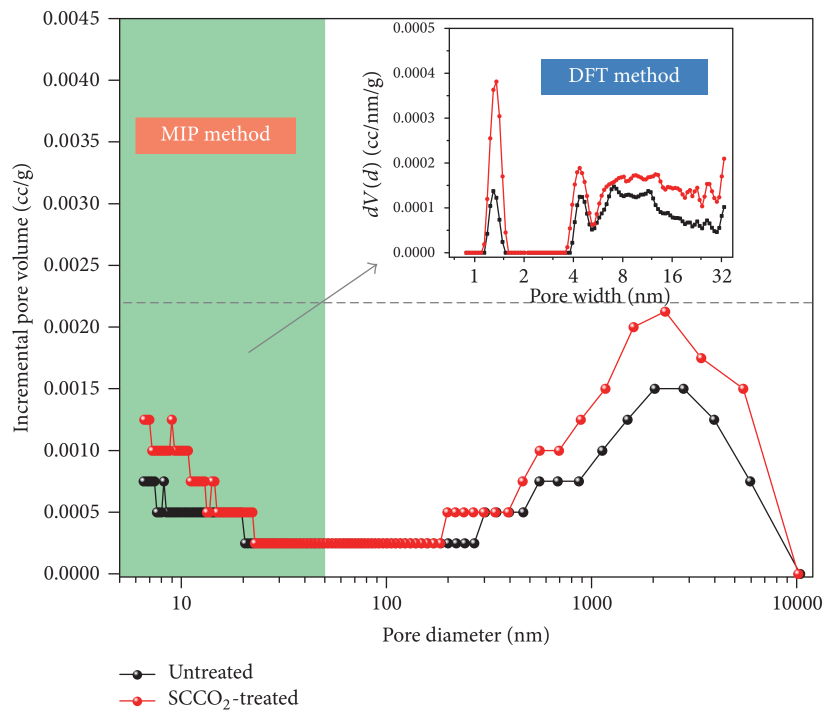

Figure 6: Pore size distribution of untreated and $SCCO_2$-treated coal from the MIP and DFT method.

of pores. Then, the injection volume of untreated and $SCCO_2$ treated oil shale shows similar trends with the same increases, which means the same amount of mercury was injected into pores before and after $SCCO_2$ treatment. Also, the changes in the ejection volume for oil shale show a decrease of 6.28% (0.00175 to 0.00164 cc/g), indicating a decrease in effective pores after $SCCO_2$ treatment. Therefore, the hysteresis loop becomes narrow with $SCCO_2$ treatment, which may result from the decrease in semiclosed pores. The reason may be attributed to adsorption-induced deformation and physical

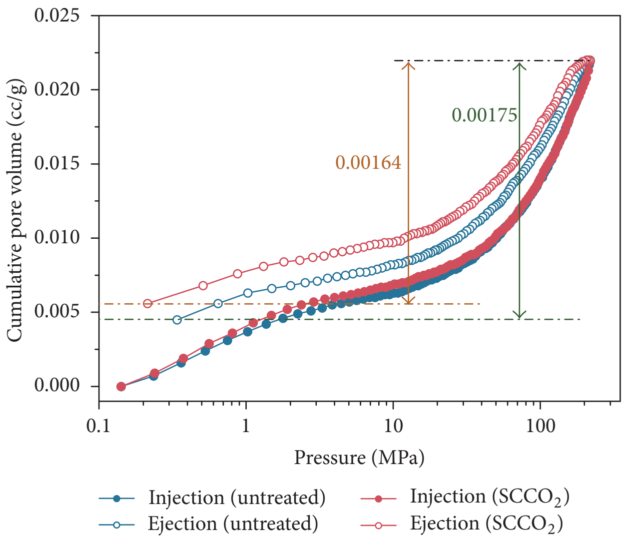

FIGURE 7: Changes in cumulative pore volume as a function of pressure for oil shale before and after $SCCO_2$ treatment by applying MIP.

constriction caused by the $SCCO_2$ dissolving and mobilizing hydrocarbons [42, 43]. Taken in conjunction with the little changes in macropores and a decrease in micropores and mesopores of oil shale as mentioned above, the results can be summarized as the decrease in the characteristics and connectivity of the pore structure related to desorption, diffusion, and seepage.

4.3. Functional Group Distribution. Infrared spectrum analysis has been widely used to study the macromolecular structure of the reservoir rocks, which is derived from the important information regarding the functional groups of organic compounds. Due to the specific molecular vibration spectrum of functional groups, the molecular structure of oil shale can be confirmed by the position and intensity of absorption peaks in the infrared spectrogram. To better understand the sealing ability of cap rocks, changes in the chemical structure of the original and $SCCO_2$ untreated oil shale above the coal reservoir were analyzed using FT-IR.

Generally, the infrared spectrum is split into the functional group region (spectral peak range: 4000–1500 cm^{-1}) and the fingerprint region (spectral peak range: 1500–400 cm^{-1}), which are shown in Figure 8. After $SCCO_2$ treatment, the absorption bands of oil shale change significantly in the region of $-CH_2$, $-CH_3$ symmetrical or antisymmetric stretching vibrations (2935–2918, 2858–2847, and 2882–2862 cm^{-1}), and $-CH_3$ antisymmetric deformation vibrations (1460–1435 cm^{-1}) in naphthenic or aliphatic bonds. Also, the spectra are characterized by a broad hydroxyl region (3697–3610 cm^{-1}), carbonyl in aldehyde, ketone, and ester (1736–1722 cm^{-1}), C–O in epoxy compounds or ethers (1330–1060 cm^{-1}), and bands in the carboxyl region (1715–1690 cm^{-1}). Moreover, the spectra contain C=C stretching vibrations of aromatic or fused rings (1635–1595 cm^{-1}), Si–O stretching vibrations (1060–1020 cm^{-1}), –SH with a peak at 475 cm^{-1}, and –S–S– with a peak at 540 cm^{-1}.

As mentioned above, the spectra, corresponding to functional groups, are grouped into three categories: (1) methyl, methylene in naphthenic, or aliphatic bonds; (2) oxygen-containing functional groups, such as hydroxyl, carbonyl, and carboxyl; (3) other functional groups. Generally, oil shale, similar to coal, has a dual pore structure that includes both matrix pores and fractures and can adsorb gas or fluids in the surface area. Thus, the first category may be thought as aliphatic and aromatic hydrocarbons in the pore structure or matrix of oil shale. The second category refers to oxygen-containing functional groups on the external surface of oil shale. The third category may be related to the silicate minerals (Si–O), organic sulfur compounds (–SH), and so on. Therefore, $SCCO_2$ may extract some hydrocarbons or other containing functional groups compounds in the matrix pores or fractures, resulting in the changes on the surface site and body structure of oil shale.

4.4. GC-MS Analysis. An investigation of the potential of $SCCO_2$ extraction was carried out for coal sample. The organic compounds, such as hydrocarbons or other substances, were presented clearly by the GC-MS detector. The partial results are exhibited in Figure 9.

According to the analysis of Chemstation software, $SCCO_2$ is capable of mobilizing small hydrocarbon molecules from the coal matrix. The hydrocarbons in the coal sample extract consisted largely of the small molecular weight *n*-alkanes, aromatic hydrocarbons (C_6H_6), and, most notably, nC_5, nC_6, nC_7, nC_8, and nC_9. These results are consistent with the research of Kolak and Burruss [21]. That is, $SCCO_2$ mobilized comparable amounts of hydrocarbons from coal sample. According to the previous studies, the $SCCO_2$ extraction of hydrocarbons is classified as aliphatic hydrocarbons and polycyclic hydrocarbons.

It has been demonstrated that hydrocarbons, existing in the macropores, mesopores, and micropores of coal structure, may generate high activation energy barriers within the coal matrix, which may hinder gas or fluids from transporting through physical constrictions. Thus, gas molecules (such as CO_2) have insufficient capacity to pass through coal beds. However, once it interacts with $SCCO_2$, hydrocarbons and mineral matter may be extracted by $SCCO_2$, contributing to reopen pores and fractures. Given the results of pore structure and GC-MS analysis, important information need to be put forward that $SCCO_2$ may facilitate coal permeability and fluid transport, resulting in the development of pore structure and migration channel of coal.

5. Discussion

5.1. Contributions of Coalbed to CO_2 Migration for Geological Sequestration. The measured CO_2 pressures in No. 2 coal seam are more than the critical pressure (7.38 MPa), and reservoir temperature of No. 2 coal seam is over critical temperature (34°C) according to the calculations, which have

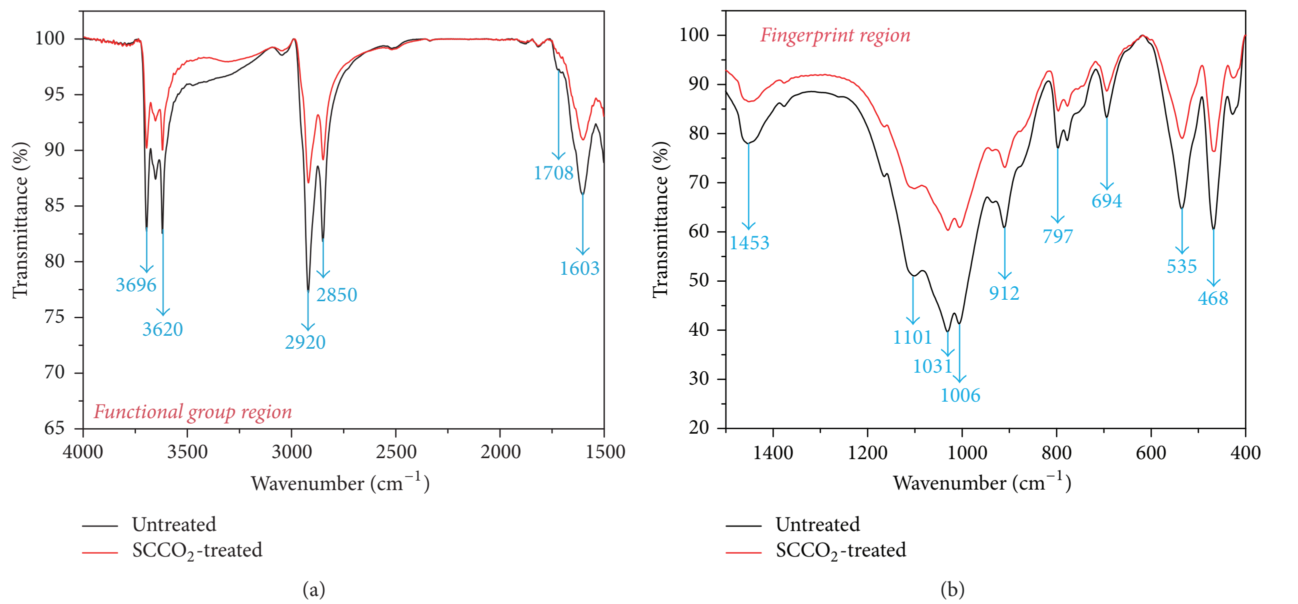

Figure 8: Infrared spectrogram of functional group region (4000–1500 cm^{-1}) and the fingerprint region (1500–400 cm^{-1}) for oil shale before and after $SCCO_2$ treatment.

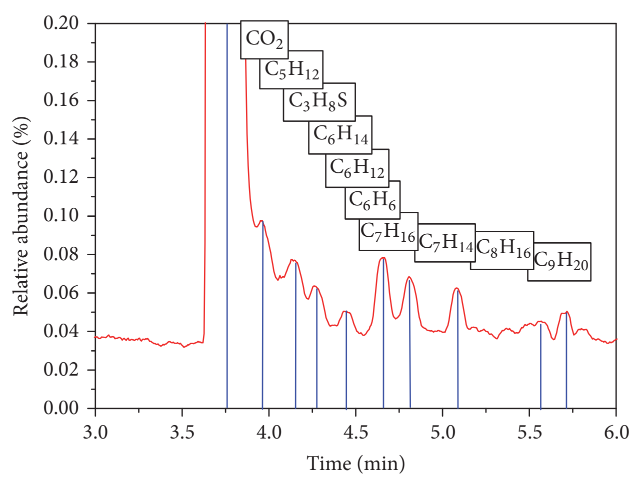

Figure 9: Relationship between relative abundance and retention time for $SCCO_2$ extraction from coal through GC-MS analysis.

been demonstrated by previous studies [44]. The investigation has confirmed that $SCCO_2$ can occur in the coal seam, even in the roof of coal seam (under cap rock) [45]. Because the source of inorganic CO_2 is derived from crust and flows along F19 faults, which will be discussed in detail in Section 5.2, CO_2 may migrate and accumulate to $SCCO_2$ in the coal seam. In this process, coal fractures may initially narrow and a decrease of permeability may occur in coal reservoir. However, the results of coal pore properties and GC-MS analysis from Figures 5–9 indicate that $SCCO_2$ enlarges the fracture width and promotes pore development by extracting hydrocarbons and mineral matter. The reasons are as follows: the migration channel, that is, fracture aperture, is a complex factor, which is related to external stress, CO_2 injection pressure, adsorption swelling effect, and SC-CO_2 extraction [46]. After a long time of evolution, an irreversible change may occur in the channel for gas diffusion and seepage, contributing to the permeability of coal reservoir [16]. Eventually, the influence of $SCCO_2$ on physical and chemical of coal may occur companied with the changes of pore structure, CH_4 displacement, and carbonate evolution after a period of CO_2 injection.

5.2. Effect of Oil Shale on Seal Capacity of CO_2 Sequestration. The findings of FTIR analysis in this study confirm that the amount of oxygen-containing functional groups were extracted from oil shale during $SCCO_2$ injection. Generally, oxygen-containing functional groups dominate the adsorption capacity through the sorption sites [47]. The decrease of oxygen-containing functional groups in oil shale may weaken the capacity of CO_2 adsorption, causing the decrease in the CO_2 sorption sites. The direct effect may cause less free CO_2 changing into adsorbed state. With migrating towards oil shale, more free CO_2 may gather beneath the cap rock. Section 5.1 has confirmed that $SCCO_2$ may facilitate the diffusion and seepage channel of coal reservoir. In this case, plenty of hydrocarbons after $SCCO_2$ extraction can move in the channel of coal bed, accompanied by free CO_2 flow. After a long injecting time, hydrocarbons will gather below oil shale. Studies indicate that hydrocarbons may restrict physical access (fractures and larger pores) to oil shale matrix [48]. A large amount of hydrocarbons and other mineral matters, existing in the oil shale structure, may have a negative effect on the permeability, which in turn can hinder CO_2 escaping from cap rock.

5.3. Implications of Tectonic Deformation on CO_2 Entrapment. Original coal seam is known to be a typical dual-porosity

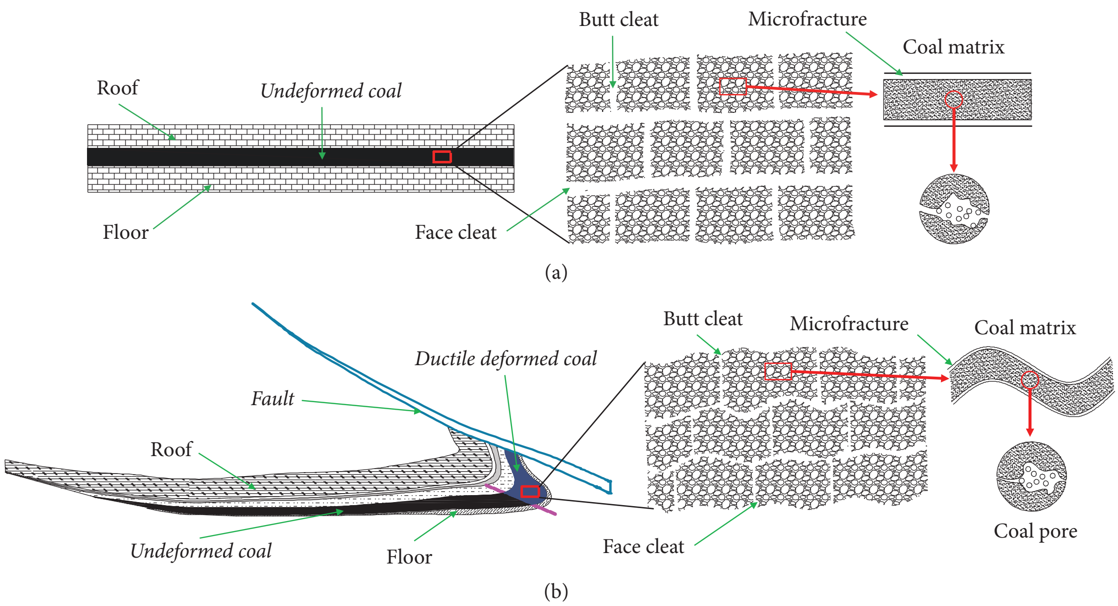

Figure 10: Influence of tectonic deformation on CO_2 entrapment in Haishiwan coalfield.

system that contains amount of coal matrix blocks divided by face cleat and butt cleat, as shown in Figure 10(a). Coal matrix, as a part of the blocks, consists of hierarchical pores with different morphology. However, because of the long-term geological formation movement, some areas may be subjected to structural changes. Taking Haishiwan coalfield as an example, undeformed coal and ductile deformed coal can be distinguished clearly in the field, which is shown in Figure 10(b). With fault tectonism, the migration of tectonic deformation may occur locally in coal seam, leading to the existence of coal reservoir and surrounding rocks. Moreover, a great quantity of winding and rub can not only produce more mylonite or other broken coals but also seal original cleats, micro-fractures, and seepage pores for CO_2 transport [49]. Therefore, poor connectivity and low permeability in the area of ductile deformed coal seam may block CO_2 migration along the bedding, which is liable to preserve more CO_2 fluids. This phenomenon serves as a role for CO_2 entrapment although geological sequestration in coal depends on multiple factors.

5.4. How to Effectively and Safely Store CO_2 in Haishiwan Coalfield. From a sequestration viewpoint, effective and safe storing in coal reservoir refers to the stable injection, migration, and storage of CO_2 in the appropriate spots for avoiding CO_2 leakage to cause Environmental Safety and Health (ES&H) issues. In Haishiwan coalfield, the favourable conditions of gas sources, migration and conduction of reservoir, sealing ability of cap rock, traps, and storage can bring about a steady environment of CO_2 gas reservoir.

According to the source and occurrence regularity of CO_2 in Yaojie coalfield as mentioned above, high concentration of CO_2 in No. 2 coal seam is derived from the indirect accumulation mode with gas production, gas guidance, gas migration, and gas storage through the brittle-ductile shear dynamic metamorphism of the active F19 fault zone [50]. Based on the analysis of F19 fault tectonic movement and CO_2 distribution in No. 2 coal seam, F19 fault played a negative role on gas source and gas storage and leads to gas entrapment during the process of CO_2 accumulation.

Large amount of inorganic CO_2, produced by the dynamic metamorphism of the active F19 fault zone, could move upwards along F19 fault and accumulate in the border of No. 2 coal seam and F19 fault. Driven by pressure gradient, CO_2 flow through the bedding orientation of No. 2 coal seam [51, 52]. With the continuous injection of CO_2, the pressure of coal reservoir increased significantly, generating $SCCO_2$ condition. The interaction between coal and $SCCO_2$ may contribute to the development of pore structure and fracture system of coal seam, which may provide conditions for the further migration. Simultaneously, CO_2 migration may provide a vector by which Polycyclic Aromatic Hydrocarbons (PAHs) and other hydrocarbons are extracted from coal matrix and transported to the direction of cap rock (oil shale) [18, 21]. These may cause the decrease in the permeability of oil shale by these substances obstructing seepage channel, which contributes to the increase in sealing capacity of oil shale [45]. Besides, oil shale and tight sandstone in the roof and floor of No. 2 coal seam have a low permeability. Also, the coal seam near cap rock may has a low permeability due to the swelling effect of CO_2 adsorption in coal matrix. The above factors may result in the CO_2 accumulation below the cap rock (the roof of No. 2 coal seam), which is exhibited in Figure 11. When CO_2 fluids transport from injection point to coal reservoir, competitive adsorption between CO_2 and CH_4 molecules occurs, leading to CH_4 desorption and migration. However, the sealing ability of cap rock (oil shale) and geological tectonism (F19 fault) contributes to gas enrichment and accumulation during a long geological time. Therefore, on-site conditions, that is, the existence of cap rock and

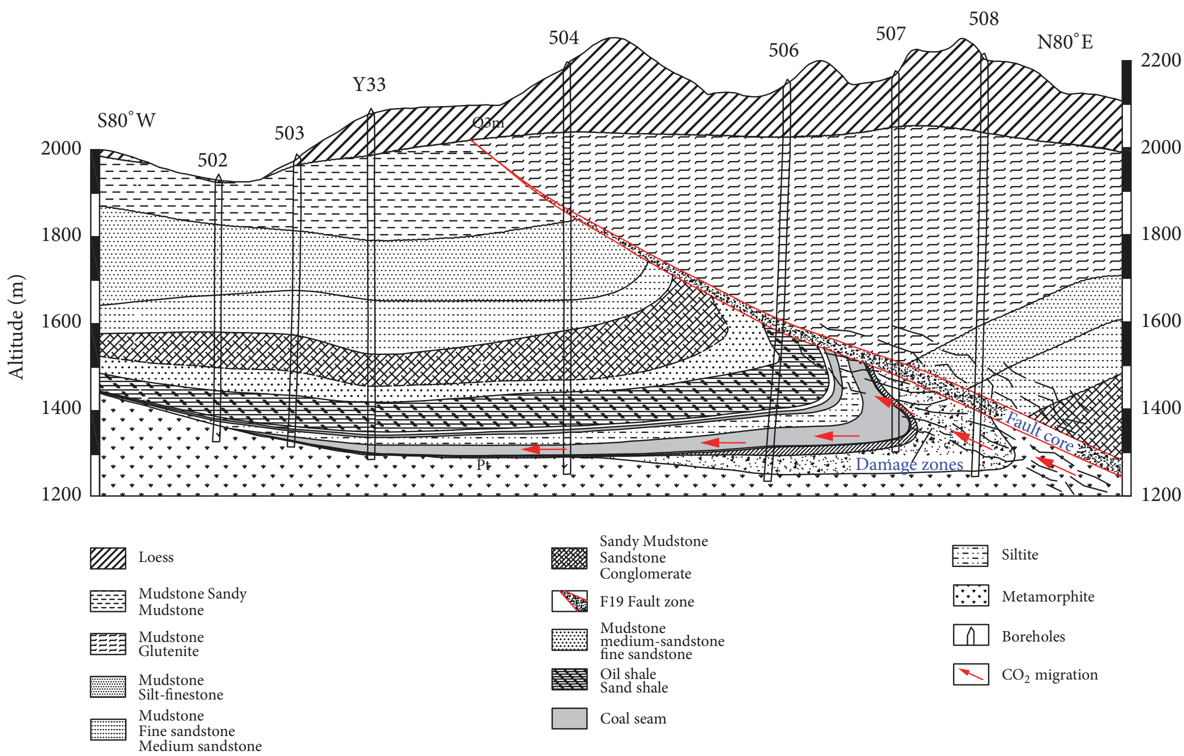

Figure 11: The mode of CO_2 enrichment and accumulation in Haishiwan coalfield.

geological tectonism, need to be considered, which have a positive implication for safe and effective CO_2 geological sequestration. The stable regional tectonic conditions and cap rock with low permeability are key factors for Haishiwan coalfield, providing an insight into the suitable selection of CCGS site.

6. Conclusions

Natural analogue studies of Haishiwan coalfield demonstrated that CO_2 can be naturally stored in deep coal seams for long period on condition that cap rock (oil shale) with good sealing capacity and stable regional tectonism, which contribute to gas entrapment and accumulation during a long geological period. Simultaneously, No. 2 coal seam, influenced by consecutive CO_2 injection and existence of $SCCO_2$, may generate amount of fractures and will facilitate fluids migration. To study the suitable selection of CCGS site, in situ conditions and experiments were investigated and analyzed through geological tectonism on reservoir properties, pore structure, functional group distributions, and $SCCO_2$ extraction. Major findings are summarized as follows.

(1) CH_4 contents increase and CO_2 contents decrease with increasing distance from F19 faults, indicating that CH_4 can be recovered after CO_2 injection. Also, higher carbonate content is closer to F19 faults, which may be derived from the transformation of CO_2 near tectonism.

(2) Changes in smaller pores and seepage-flow pores (mesopores and macropores) are facilitated by $SCCO_2$, but macropores in oil shale show no significant change and a slight decrease in micropores and mesopores was found after $SCCO_2$ treatment. Thus, transport in coal matrix and seepage ability of coal seam will be promoted. Meanwhile, changes in pore structure properties of oil shale can lead to a low permeability and connectivity, which hinder the movement of fluid desorption, diffusion, and seepage.

(3) For FTIR analysis, amount of matters containing hydrocarbons or functional groups compounds in oil shale matrix are mobilized by $SCCO_2$, causing the changes on the surface site and body structure. Then, aliphatic hydrocarbons and polycyclic hydrocarbons obtained from $SCCO_2$ extraction enhance the development of pore structure of coal, generating more migration channel.

Conflicts of Interest

The authors declare no competing financial interests.

Acknowledgments

The authors are grateful to the Fundamental Research Funds for the Central Universities (Grant no. 2015XKMS006) and the Priority Academic Program Development of Jiangsu Higher Education Institutions (PAPD).

References

[1] G. Aydin, I. Karakurt, and K. Aydiner, “Evaluation of geologic storage options of CO2: applicability, cost, storage capacity and safety,” *Energy Policy*, vol. 38, no. 9, pp. 5072–5080, 2010.

[2] E. Bryant, *Climate process and change*, Cambridge University Press, 1997.

[3] BP. Company, *BP statistical review of world energy*, British Petroleum Company, London, England, 2017.

[4] ME. Boot-Handford, JC. Abanades, EJ. Anthony, MJ. Blunt, S. Brandani, N. Mac Dowell et al., "Carbon capture and storage update," *Environmental Science*, vol. 7, no. 1, pp. 130-89, 2014.

[5] W. Chen and R. Xu, "Clean coal technology development in China," *Energy Policy*, vol. 38, no. 5, pp. 2123–2130, 2010.

[6] J. Koornneef, A. Ramírez, W. Turkenburg, and A. Faaij, "The environmental impact and risk assessment of CO2 capture, transport and storage - An evaluation of the knowledge base," *Progress in Energy and Combustion Science*, vol. 38, no. 1, pp. 62–86, 2012.

[7] C. M. White, D. H. Smith, K. L. Jones et al., "Sequestration of carbon dioxide in coal with enhanced coalbed methane recovery—a review," *Energy & Fuels*, vol. 19, no. 3, pp. 659–724, 2005.

[8] S. Bachu, "CO2 storage in geological media: role, means, status and barriers to deployment," *Progress in Energy and Combustion Science*, vol. 34, no. 2, pp. 254–273, 2008.

[9] J. Li, X. Liang, T. Cockerill, J. Gibbins, and D. Reiner, "Opportunities and barriers for implementing CO 2 capture ready designs: a case study of stakeholder perceptions in Guangdong, China," *Energy Policy*, vol. 45, pp. 243–251, 2012.

[10] N. P. Qafoku, A. R. Lawter, D. H. Bacon, L. Zheng, J. Kyle, and C. F. Brown, "Review of the impacts of leaking CO2 gas and brine on groundwater quality," *Earth-Science Reviews*, vol. 169, pp. 69–84, 2017.

[11] M. M. Faiz, A. Saghafi, S. A. Barclay, L. Stalker, N. R. Sherwood, and D. J. Whitford, "Evaluating geological sequestration of CO2 in bituminous coals: The southern Sydney Basin, Australia as a natural analogue," *International Journal of Greenhouse Gas Control*, vol. 1, no. 2, pp. 223–235, 2007.

[12] W. Li, Y.-P. Cheng, and L. Wang, "The origin and formation of CO2 gas pools in the coal seam of the Yaojie coalfield in China," *International Journal of Coal Geology*, vol. 85, no. 2, pp. 227–236, 2011.

[13] Q. Li, D. Kuang, G. Liu, and X. Liu, "Acid gas injection: a suitability evaluation for the sequestration site in Amu Darya Basin," *Geol Rev*, 2014.

[14] Y. Yang, M. Jinfeng, and L. Lin, "Research progress of 4D multicomponent seismic monitoring technique in carbon capture and storage," *Advances in Earth Science*, vol. 30, no. 10, pp. 1119-26, 2015.

[15] A. Raza, R. Rezaee, R. Gholami, C. H. Bing, R. Nagarajan, and M. A. Hamid, "A screening criterion for selection of suitable CO2 storage sites," *Journal of Natural Gas Science and Engineering*, vol. 28, pp. 317–327, 2016.

[16] P. Massarotto, S. D. Golding, J.-S. Bae, R. Iyer, and V. Rudolph, "Changes in reservoir properties from injection of supercritical CO2 into coal seams - a laboratory study," *International Journal of Coal Geology*, vol. 82, no. 3-4, pp. 269–279, 2010.

[17] S. Day, R. Fry, and R. Sakurovs, "Swelling of Australian coals in supercritical CO2," *International Journal of Coal Geology*, vol. 74, no. 1, pp. 41–52, 2008.

[18] J. W. Larsen, "The effects of dissolved CO2 on coal structure and properties," *International Journal of Coal Geology*, vol. 57, no. 1, pp. 63–70, 2004.

[19] C. C. Giri and D. K. Sharma, "Mass-transfer studies of solvent extraction of coals in N-methyl-2-pyrrolidone," *Fuel*, vol. 79, no. 5, pp. 577–585, 2000.

[20] P. Painter, M. Starsinic, and M. Coleman, "Determination of functional groups in coal by Fourier transform interferometry," *Fourier Transform Infrared Spectroscopy*, pp. 169–240, 2012.

[21] J. J. Kolak and R. C. Burruss, "Geochemical investigation of the potential for mobilizing non-methane hydrocarbons during carbon dioxide storage in deep coal beds," *ENERGY & FUELS*, vol. 20, no. 2, pp. 566–574, 2006.

[22] O. Bildstein, C. Kervévan, V. Lagneau et al., "Integrative modeling of caprock integrity in the context of CO2 storage: evolution of transport and geochemical properties and impact on performance and safety assessment," *Oil & Gas Science and Technology - Revue d'IFP Energies nouvelles*, vol. 65, no. 3, pp. 485–502, 2010.

[23] T. Zhao, Y. Zhang, Q. Li, Z. Li, and J. Qi, "Lanzhou-Minhe basin tectonics and new tectonic movement related disasters discussion," *Northwestern geology*, p. 33, 2000.

[24] L. Wang, Y. Cheng, and W. Li, "Migration of metamorphic CO2 into a coal seam: a natural analog study to assess the long-term fate of CO2 in Coal Bed Carbon Capture, Utilization, and Storage Projects," *Geofluids*, vol. 14, no. 4, pp. 379–390, 2014.

[25] M. Tao, *Geochemical and structural characteristics of carbon dioxide outburst in Yaojie Coal Mine: PhD thesis, Lanzhou institute of geology, Chinese academy of science [Ph.D. thesis]*, China, 1993.

[26] K. D. O'Hara, "Fluid-rock interaction in crustal shear zones: a directed percolation approach," *Geology*, vol. 22, no. 9, pp. 843–846, 1994.

[27] K. O'Hara and W. H. Blackburn, "Volume-loss model for trace-element enrichments in mylonites," *Geology*, vol. 17, no. 6, pp. 524–527, 1989.

[28] JJ. Kolak and RC. Burruss, "An organic geochemical assessment of CO2-coal interactions during sequestration," in *US Geological Survey Open-File Report*, pp. 03–453, 2003.

[29] H. Hellevang, P. Aagaard, E. H. Oelkers, and B. Kvamme, "Can dawsonite permanently trap CO2?" *Environmental Science & Technology*, vol. 39, no. 21, pp. 8281–8287, 2005.

[30] J.-Q. Shi and S. Durucan, "Gas Storage and Flow in Coalbed Reservoirs: Implementation of a Bidisperse Pore Model for Gas Diffusion in Coal Matrix," in *SPE Annual Technical Conference and Exhibition: Society of Petroleum Engineers*, pp. 2495–2503, USA, October 2003.

[31] Y. Yao, D. Liu, D. Tang et al., "Fractal characterization of seepage-pores of coals from China: an investigation on permeability of coals," *Computers & Geosciences*, vol. 35, no. 6, pp. 1159–1166, 2009.

[32] M. Thommes, K. Kaneko, A. V. Neimark et al., "Physisorption of gases, with special reference to the evaluation of surface area and pore size distribution (IUPAC Technical Report)," *Pure and Applied Chemistry*, vol. 87, no. 9-10, pp. 1051–1069, 2015.

[33] S. Brunauer, P. H. Emmett, and E. Teller, "Adsorption of gases in multimolecular layers," *Journal of the American Chemical Society*, vol. 60, no. 2, pp. 309–319, 1938.

[34] E. P. Barrett, L. G. Joyner, and P. P. Halenda, "The determination of pore volume and area distributions in porous substances. I. Computations from nitrogen isotherms," *Journal of the American Chemical Society*, vol. 73, no. 1, pp. 373–380, 1951.

[35] A. V. Neimark, Y. Lin, P. I. Ravikovitch, and M. Thommes, "Quenched solid density functional theory and pore size analysis of micro-mesoporous carbons," *Carbon*, vol. 47, no. 7, pp. 1617–1628, 2009.

[36] G. Y. Gor, M. Thommes, K. A. Cychosz, and A. V. Neimark, "Quenched solid density functional theory method for characterization of mesoporous carbons by nitrogen adsorption," *Carbon*, vol. 50, no. 4, pp. 1583–1590, 2012.

[37] M. Thommes and K. A. Cychosz, "Physical adsorption characterization of nanoporous materials: Progress and challenges," *Adsorption*, vol. 20, no. 2-3, pp. 233–250, 2014.

[38] P. Psarras, R. Holmes, V. Vishal, and J. Wilcox, "Methane and CO2 Adsorption Capacities of Kerogen in the Eagle Ford Shale from Molecular Simulation," *Accounts of Chemical Research*, vol. 50, no. 8, pp. 1818–1828, 2017.

[39] R. Holmes, E. C. Rupp, V. Vishal, and J. Wilcox, "Selection of shale preparation protocol and outgas procedures for applications in low-pressure analysis," *Energy & Fuels*, vol. 31, no. 9, pp. 9043–9051, 2017.

[40] K. Zhang, Y. Cheng, K. Jin et al., "Effects of supercritical CO2 fluids on pore morphology of coal: implications for CO2 geological sequestration," *Energy & Fuels*, vol. 31, no. 5, pp. 4731–4741, 2017.

[41] K. Yang, X. Lu, Y. Lin, and A. V. Neimark, "Effects of CO2 adsorption on coal deformation during geological sequestration," *Journal of Geophysical Research: Solid Earth*, vol. 116, no. 8, Article ID B08212, 2011.

[42] J.-S. Bae, S. K. Bhatia, V. Rudolph, and P. Massarotto, "Pore accessibility of methane and carbon dioxide in coals," *Energy & Fuels*, vol. 23, no. 6, pp. 3319–3327, 2009.

[43] T. X. Nguyen and S. K. Bhatia, "Determination of pore accessibility in disordered nanoporous materials," *The Journal of Physical Chemistry C*, vol. 111, no. 5, pp. 2212–2222, 2007.

[44] D. Wu and Y. Cheng, "The experimental study of the impact on supercritical CO_2 from CH_4 composition in coal," in *Proceedings of the 11th Underground Coal Operators' Conference*, pp. 277–284, University of Wollongong & the Australasian Institute of Mining and Metallurgy, 2011.

[45] W. Li, Y. Cheng, L. Wang, H. Zhou, and H. Wang, "Evaluating the security of geological coalbed sequestration of supercritical CO2 reservoirs: the Haishiwan coalfield, China as a natural analogue," *International Journal of Greenhouse Gas Control*, vol. 13, pp. 102–111, 2013.

[46] K. Zhang, Y. Cheng, W. Li, D. Wu, and Z. Liu, "Influence of supercritical CO2 on pore structure and functional groups of coal: implications for CO2 sequestration," *Journal of Natural Gas Science and Engineering*, vol. 40, pp. 288–298, 2017.

[47] Y. Liu and J. Wilcox, "Effects of surface heterogeneity on the adsorption of CO2 in microporous carbons," *Environmental Science & Technology*, vol. 46, no. 3, pp. 1940–1947, 2012.

[48] J. J. Kolak, P. C. Hackley, L. F. Ruppert, P. D. Warwick, and R. C. Burruss, "Using ground and intact coal samples to evaluate hydrocarbon fate during supercritical CO2 injection into coal beds: effects of particle size and coal moisture," *Energy & Fuels*, vol. 29, no. 8, pp. 5187–5203, 2015.

[49] H. Li, Y. Ogawa, and S. Shimada, "Mechanism of methane flow through sheared coals and its role on methane recovery," *Fuel*, vol. 82, no. 10, pp. 1271–1279, 2003.

[50] W. Li, P. L. Younger, Y. Cheng et al., "Addressing the CO2 emissions of the world's largest coal producer and consumer: Lessons from the Haishiwan Coalfield, China," *Energy*, vol. 80, pp. 400–413, 2015.

[51] F. Anggara, K. Sasaki, S. Rodrigues, and Y. Sugai, "The effect of megascopic texture on swelling of a low rank coal in supercritical carbon dioxide," *International Journal of Coal Geology*, vol. 125, pp. 45–56, 2014.

[52] P. N. K. De Silva and P. G. Ranjith, "Understanding the significance of in situ coal properties for CO2 sequestration: an experimental and numerical study," *International Journal of Energy Research*, vol. 38, no. 1, pp. 60–69, 2014.